Journal of Nanotechnology and Nanobiotechnology

Research

Effect of Selenium Vapor Pressure on the Growth of 2D Ge-Doped GaSe by Low-Temperature Liquid Phase Deposition

Yohei Sato[*], Chao Tang, Katsuya Watanabe, Tadao Tanabe and Yutaka Oyama
Department of Materials Science and Engineering, Tohoku University, Aramaki-Aza Aoba 6-6-11-1021, Sendai 980-8579, Japan

[*]**Corresponding author:** Yohei Sato, Department of Materials Science & Engineering, Graduate School of Engineering, Tohoku university, Aoba-ku Aramaki-aza aoba 6-6-11-1021 Sendai 980-8579, Japan, Tel: 022-795-7330; Fax: 022-795-7329; E-mail: s.yohei@dc.tohoku.ac.jp

Received: Mar 02 2024, **Accepted:** Apr 24 2024; **Published:** Apr 26, 2024, DOI: 10.59462/jnnb.1.1.103

Citation: Sato Y, Tang C, Watanabe K, Tanabe T, OyamaY (2024) Effect of Selenium Vapor Pressure on the Growth of 2D Ge-Doped GaSe by Low-Temperature Liquid Phase Deposition. Journal of Nanotechnology and Nanobiotechnology, 1(1):103.

Abstract

Two dimensional (2D) germanium (Ge)-doped single crystal gallium selenide (GaSe) grown by the Temperature Difference Method under a Controlled Vapor Pressure (TDM-CVP) has been used in the development of highly efficient terahertz (THz) light sources. In this article, we compare the electrical properties, lattice constant and THz transparency of Ge-doped GaSe (GaSe:Ge) with those of nominally undoped GaSe. By doping with Ge, the carrier concentration was reduced to 1/6 of the value for undoped GaSe (Nominally undoped GaSe $p = 3.2\times(10)^{15}$ cm^{-3} at 255 K, GaSe:Ge $p = 4.9\times(10)^{14}$ cm^{-3} at 255 K). At the same time, the lattice constant increased and the absorption coefficient α at frequencies less than 2.4 THz decreased (Nominally undoped GaSe $\alpha=24$ cm^{-1} at 2.17 THz, GaSe:Ge $\alpha=22$ cm^{-1} at 2.17 THz). Initially, the lattice constant of GaSe:Ge increased as the applied Se vapor pressure was increased and then decreased when higher Se vapor pressure was applied. From these results, we consider that the Ge atoms occupy Se sites and this promotes the recombination of free carriers and suppresses free carrier absorption. These are important factors for highly efficient generation in the low THz frequency range.

Keywords Temperature difference method; THz frequency; Se vapor pressure

Introduction

Gallium Selenide (GaSe) is one of the most promising layered chalcogenide semiconductors for future novel semiconductor devices. The electrical and optical characteristics of two-dimensional (2D) GaSe, which has a finite energy bandgap, are very appealing. As such, GaSe has been extensively studied. For example, there has been research done on the interlayer van der Waals bonding force [1], and its uses as a THz wave light source [2] and for spin-field-effect transistors [3].

Because of its extremely asymmetric layered crystal structure, GaSe has a relatively high second order nonlinear optical (NLO) constant (d_{22}=54 pm/V)[4]. Therefore, THz radiation can be generated from GaSe crystals via the difference frequency generation (DFG) process, which is a second order NLO effect. In addition, crystalline GaSe is widely transparent from infrared (IR) to THz and it is theoretically possible to generate THz radiation from sub-THz to mid-IR (0.1~100 THz) via DFG using GaSe crystals [5]. Furthermore, because GaSe, which is a layered 2D semiconductor, has high birefringence [6], it is possible to apply collinear phase matching for THz wave generation via DFG and improvement of the conversion coefficient is expected utilizing DFG [5,7].

Commercially available GaSe crystals are grown from high temperature melts by the Bridgman method. However, Bridgman grown GaSe crystals have structural disorders, such as two polytypes (γ and ε type) mixed together and thermal equilibrium point defects due to the high temperature growth at the melting point of GaSe (938°C) [8]. In addition, there is a problem with the stoichiometry due to the dissociation of Se during crystal growth as a result of the vapor pressure of Se being higher than that of Ga. These structural disorders and the nonstoichiometry lead to a reduction in transparency in the IR & THz frequency ranges [9] and reduce the conversion efficiency of the DFG process. Using the Temperature Difference Method under a Controlled Vapor Pressure (TDM-CVP) we succeeded in selectively growing single ε -type GaSe and reduced the THz absorption compared with the nonstoichiometric crystals grown by the Bridgman method [10,11]. TDM-CVP utilizes a temperature gradient in the Ga-Se solution and enables fixed low temperature growth at temperatures 200°C lower than the melting point of GaSe. Therefore, high purity crystal can be grown because contamination of the solution from growth container is small due to low temperature growth. Furthermore, it is possible to control the stoichiometry of GaSe by controlling the Se vapor pressure applied to the Ga-Se solution during crystal growth [10]. Compared with GaSe crystals grown by the Bridgman method, the transparency of GaSe crystals grown by TDM-CVP is higher in the near IR (λ=1 μm) and high THz frequency ranges (>2.4 THz) [11]. In addition, the conversion efficiency for DFG using crystals grown by TDM-CVP was 1.2×10^{-6} j^{-1}, which is greater than the 3.0×10^{-7} j^{-1} achieved with Bridgman grown crystals [12]. It is expected that these improvements in transparency and conversion efficiency are due to the improved crystallinity of GaSe obtained using TDM-CVP.

However, free carrier absorption of THz waves in the low THz frequency range is a serious problem in GaSe crystals grown by TDM-CVP [11]. In order to suppress this, it is necessary to reduce the free carrier concentration. We previously succeeded in reducing the free carrier concentration and suppressing the free carrier absorption by using the transition metal Ti [13]. In this paper, GaSe is doped with the group IV amphoteric impurity Ge in order to reduce the concentration of holes, which is the majority carrier, and thereby suppress free carrier absorption in the low THz frequency range. If group III Ga atoms and group VI Se atoms are substituted by group IV Ge atoms, donors and double acceptors, respectively, are formed. The double acceptors are expected to introduce deep levels, which give rise to carrier recombination and compensation. If Ga or Se atoms are substituted by Ge atoms, the hole concentration is reduced by compensation or recombination, respectively.

In this work, we characterized nominally undoped and Ge-doped GaSe crystals grown by TDM-CVP. Furthermore, we examined the effects of the Ge doping and the applied Se vapor pressure on the crystal structure and the electrical properties using highly accurate XRD measurements and temperature dependent Hall effect measurements. Finally, in order to evaluate the effect of doping with Ge on the transparency of the crystal, the THz transmittance was measured in the low THz frequency range.

Materials and Methods

Crystal growth

A schematic view of the equipment used for the crystal growth is shown in Figure 1. The quartz ampoule, crucible and rod were dipped in sulfuric acid after washing with acetone to remove organic matter. Then, Ga, Se, and the dopant material Ge were placed in the quartz crucible. The purities of the Ga and Se were 6N and 7N, respectively. The resistivity of the Ge was 45–48 Ω·cm and its conduction type was n-type. The quartz crucible, quartz rod and metal Se were inserted into the quartz ampoule and this was evacuated and sealed at 10-6 Torr. The temperature in the ampoule was controlled by 4 zone heaters as shown in Figure 1. The growth process was as follows. First, supersaturation was induced in the Ga-Se solution by diffusion of the Se to the bottom of the crucible due to the temperature gradient. Then, the GaSe crystal was segregated by resolution of the supersaturation.

The quartz rod was set at the bottom of the ampoule, which enabled the path of the Se vapor to be narrower than the mean free path. The Se vapor pressure in the space around the quartz rod is determined by the temperature. This relationship is expressed by

$$_{H} = _{Se} \sqrt{G/V} \text{ [14]..........(1)}$$

Furthermore, the relationship between the vapor pressure P_{Se} and the vapor control temperature T_V at the bottom of the ampoule is expressed by

$$\log_{Se}(\text{atm}) = -5043/_{V}(\text{K}) + 5.265 \text{[15,16] ....(2)}$$

Combining equations (1) and (2), gives the following expression for the applied Se vapor pressure P_H.

$$_{H} = 10^{-5043/_{V}(\text{K}) + 5.265} \sqrt{G/V} \text{ ....(3)}$$

According to Equation (3), controlling the temperature in the ampoule enables control of the applied Se vapor pressure. Using this control, the stoichiometry of the crystal can be controlled.

The growth conditions for the GaSe crystals are shown in Table 1. Evaluation of the samples was done using XRD, Hall Effect measurements and THz transmittance measurements.

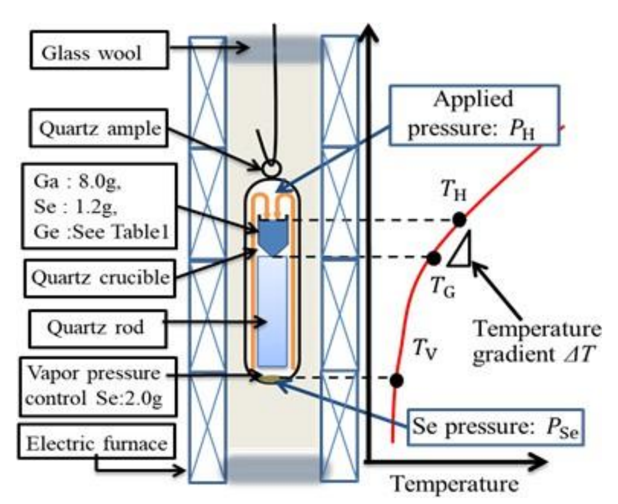

Figure 1: Schematic view of the equipment for TDM-CVP.

Growth conditions	A	B	C	D	E	F	G	H	I	J
Ge concentration (at%)	0.0	0.0	0.5	0.50	0.50	0.75	0.75	0.75	1.0	2.0
T(°C /cm)	10	10	10	11	10	10	10	10	12	10
TH(°C)	700	670	670	673	670	676	670	670	676	670
TG(°C)	670	640	640	640	640	640	640	640	640	640
PH(Torr)	230	58	12	159	376	12	81	376	164	81
Growth time (days)	14	14	14	21	14	14	14	14	14	14

Table 1: Growth conditions for GaSe crystals.

Evaluation

XRD measurements: GaSe crystal has hexagonal structure and its crystal structure is shown in Figure 2. Lattice constant c perpendicular to the layer is 15.95 Å and lattice constant a parallel to the layer is 3.755 Å. The space group of ε-GaSe is $P\bar{6}2$ [15,16]. The dependences of the lattice constant along c-axis on the Ge concentration and the applied Se vapor pressure were evaluated for the nine samples from B to J. For this, we conducted highly accurate XRD measurements (X'Pert3 MRD PANalytical Inc.) using X-rays from the CuKα1 line (λ=0.154056 nm). Ge (220) crystals on the incident and detection sides made the X-rays monochromatic and parallel. Calibration of the XRD equipment without a sample was done with 2θ=0°. The lattice constant along c-axi s is calculated from the symmetric diffraction.

Symmetric X-ray diffraction patterns of samples B and C from 0 0 l were measured by D8 ADVANCE (Bruker AXS Co., Ltd) with CuK_α radiation and shown in Figure 3. From the Brag's law, the value of lattice constant and distance between the plane are more accurately calculated from the diffraction on the high angle side. However, in the highly accurate XRD measurements, diffraction intensities from 0 0 12 and 0 0 14 were not enough to calculate the lattice constant.

Therefore, using the accurate XRD measurement equipment (X'Pert3 MRD PANalytical Inc.), lattice constant c is calculated from the 0 0 10 diffraction peak.

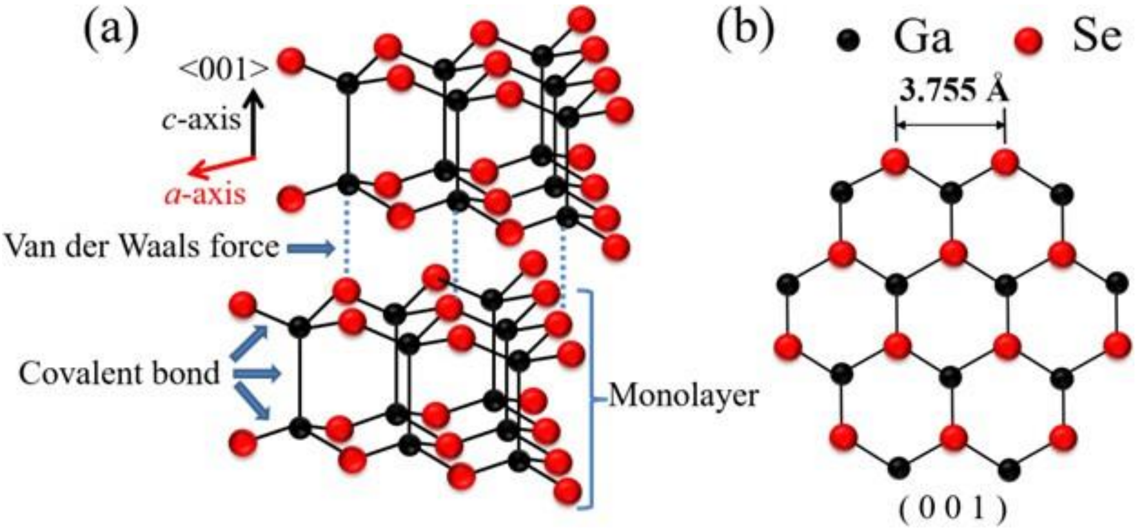

Figure 2: (a) Schematic view of GaSe crystal structure and (b) (001) of GaSe crystal.

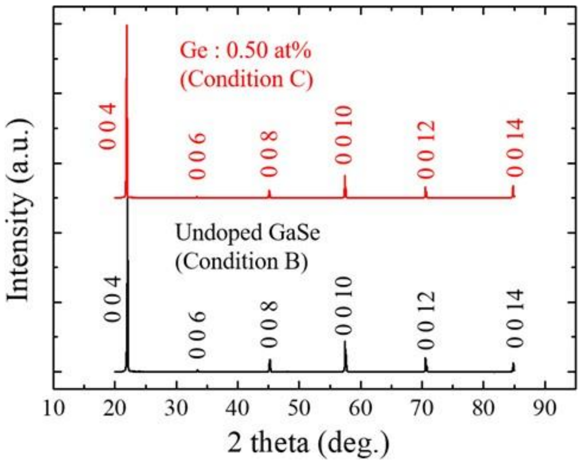

Figure 3: Patterns of symmetric X-ray diffraction from (0 0 l) for sample B and C.

Hall effect measurements: The temperature dependent carrier concentrations of samples A and D in Table 1 were evaluated by Hall effect measurements (Resitest8300 TOYOTECHNICA Inc.) in the dark. Carrier concentration p is measured by Van der Pauw method and calculated each temperature by the following equation.

$$[\mathrm{cm}^{-3}] = \frac{1}{[\cdot]}\,\frac{{}_{\mathrm{H}}[\mathrm{V}]\cdot[\mathrm{m}]}{[\mathrm{A}]\cdot[\mathrm{T}]}\,10^{-6} \quad ....(4)$$

In Equation (4), e is elementary charge, V_H is Hall voltage, t is the sample thickness in the direction of the magnetic field (Sample A : 3.80×10^{-4} m, Sample B : 2.25×10^{-4} m), I is the current passed through the sample (1.0×10^{-4} A) and B is the applied magnetic field ($0.6\ \mathrm{T} = 0.6\ \mathrm{V \cdot s \cdot m^{-2}}$).

In order to form an ohmic contact to the crystals, indium was placed on the crystal surface after the pealing of the sample, then annealed for 10 minute at 250°C in N_2.

THz transmittance measurements: Transmittance measurements in the frequency range of 2–3 THz were done on samples B and C using a frequency tunable THz source. Figure 4 shows a schematic of the experimental setup for the measurements. The pump source and signal source for DFG were both Cr:Foresterite lasers excited by a two channel Nd:YAG laser (LOTIIS inc.). The wavelengths were 1203 nm and 1230 nm ~ 1264 nm, respectively. The light from these lasers was mixed in a GaP crystal under controlled phase matching conditions. The GaSe sample was irradiated with THz waves generated in the GaP crystal and the THz transmittance was measured. The thickness of samples B and C were 291 µm and 233 µm, respectively. In order to make the surface of samples flat, these were peeled using tape. The absorption coefficient α was calculated using Equation (5) with thickness of the sample d and transmittance T.

$$(\mathrm{cm}^{-1}) = -\frac{1}{}\ln \quad ....(5)$$

T is expressed by

$$= \frac{}{{}_{0}(1-)} \quad ....(6)$$

where I and I_0 are the intensities of the transmitted and irradiated THz waves, respectively. The reflection at the irradiated surface was calculated and eliminated from the transmittance calculations. The reflectance was calculated from

$$= \left(\frac{\mathrm{Air} - \mathrm{GaSe}}{\mathrm{Air} - \mathrm{GaSe}}\right)^2 \ldots\ldots\ldots.(7)$$

where the refractive index of air $n_{air} = 1$ and the refractive index of GaSe n_{GaSe} was calculated from the Sellmeier equation [6].

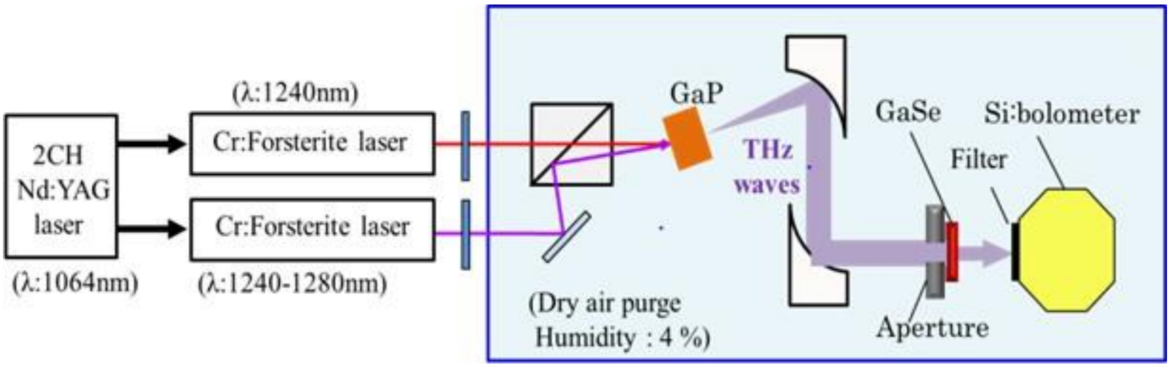

Figure 4: Experimental setup for THz transmittance measurements.

Results and Discussion

XRD measurements

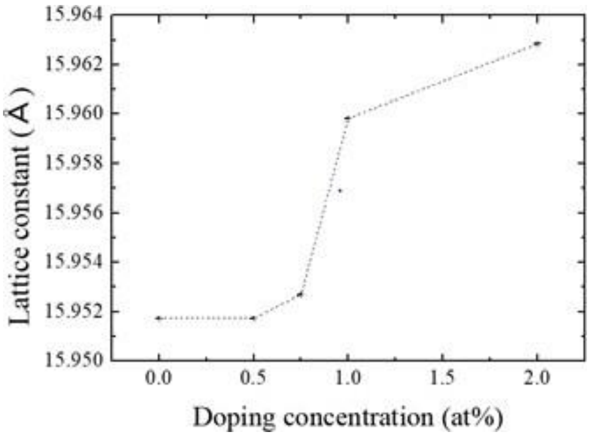

Figure 5: 0 0 10 symmetric diffraction peaks.

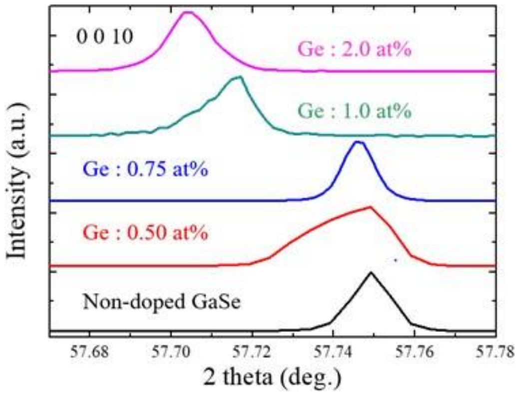

Figure 6: Lattice constant of GaSe for each Ge doping concentration.

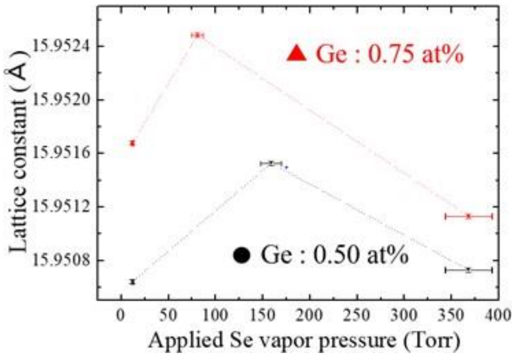

Figure 7: Applied Se vapor pressure dependence of the lattice constant constant of GaSe for each Ge doping concentration.

Figure 5, shows the rocking curves for 0 0 10 symmetric diffraction for samples with different doping concentrations (B, D, G, I and J). Figure 6, shows the dependence of the lattice constant on the Ge doping concentration calculated from the 2θ position of the peak in Figure 5. In Figures 6 and 7, error bars of lattice constant value are calculated from accuracy of the XRD measurement equipment and error bars of doping concentration value are calculated from the accuracy of the material weight measured by electronic balance. As shown in Figure 6, the lattice constant of the GaSe crystal increases with increasing Ge doping concentration. This result indicates that doping with Ge expands the structure of GaSe. The Ge in GaSe either forms precipitates, replaces Ga or Se atoms in substitutional sites, or falls into interstitial sites. Because the covalent radius of Ge (1.22 Å) is smaller than that of Ga (1.26 Å) and larger than that of Se (1.14), it is considered that Ge occupies Se sites or interstitial sites or precipitates. Figure 7 shows the lattice constant of GaSe:Ge(0.5at% & 0.75at%) for each applied Se vapor pressure during crystal growth. In Figure 6, error bars of applied Se vapor pressure value are calculated from accuracy of temperature measured by the thermocouple. As shown in Figure 7, the lattice constant of GaSe:Ge(0.5at% & 0.75at%) increases and then decreases as the applied Se vapor pressure is increased. This suggests that there are Se vacancies and substituent Ge atoms in the GaSe structure, and at low Se vapor pressure the lattice constant increases as the number of Se vacancies decreases. On the other hand, at high Se vapor pressure, there are no Se vacancies in the GaSe crystal and the lattice constant decreases due to Ge substituents at Se sites. From the above XRD measurement results, because Ge expands the crystal structure and the lattice constant of GaSe:Ge decreases with the reduction in Se vacancies at high Se vapor pressures, it is considered that the Ge atoms occupy Se sites.

Hall effect measurements

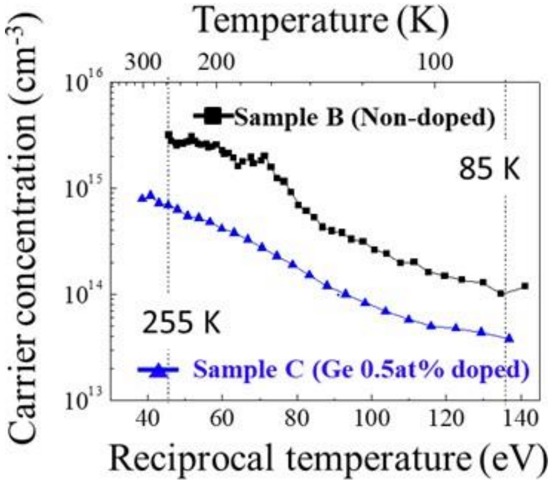

Figure 8:Temperature dependent carrier concentration of samples A and D.

Doped Ge concentration (at%) in the Ga solution	0	0.5
Carrier concentration (cm^{-3})	$3.2*10^{15}$	$5.6*10^{14}$
Temperature (K)	254	255

Table 2: Carrier concentration of undoped and Ge doped GaSe crystal.

Figure 8, shows the temperature dependent carrier concentration of samples A and D measured by Hall effect measurements. From these measurements, it was confirmed that the conduction type of GaSe doped with 0.5at% Ge is p-type and that a shallow acceptor level (EV + 15meV) is formed in the bandgap as well as in the nominally undoped GaSe. Compared with the undoped GaSe, the carrier concentration of GaSe doped with 0.5at% Ge is smaller in the temperature range from 80 K – 300 K. As shown in the Table 2, The carrier concentration of GaSe doped with 0.5at% Ge at 255 K ($p = 5.6 \times 10^{14}$ cm^{-3}) was about 1/6 of that for undoped GaSe at 254 K ($p = 3.2 \times 10^{15}$ cm^{-3}). Because the results of the XRD measurements suggest that the substituent Ge atoms are at Se sites, group IV Ge atoms form double acceptors which create a deep level promoting recombination of the free carriers.

THz transmittance measurements

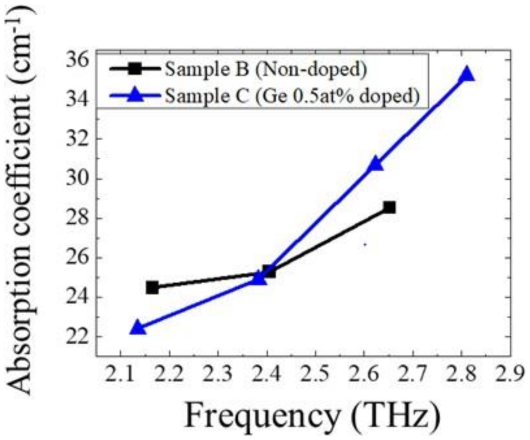

Figure 9: Absorption coefficient of samples B and C in the frequency range of 2 ~ 3 THz.

Figure 9, shows the absorption coefficient of samples B and C. There are interference patterns in the as-measured spectra, so the symbols plotted show the average absorption coefficient between the peaks and troughs in the interference patterns. As shown in Figure 8, below 2.4 THz, the absorption coefficient of GaSe doped with 0.5 at% Ge is less than that of the undoped sample. Therefore, it is considered that the transparency in the low THz frequency range improves with Ge doping and free carrier absorption is suppressed. However, above 2.4 THz, the absorption coefficient of doped GaSe is larger than that of undoped GaSe. This is considered to be because sample C was grown at a low applied Se vapor pressure (12 Torr), and that there is phonon absorption of the THz radiation due to the nonstoichiometric composition above 2.4 THz [11].

Conclusion

We succeeded in growing GaSe crystals doped with different amounts of Ge using TDM-CVP at various applied Se vapor pressures. The lattice constant of the crystal perpendicular to the direction of the layers increased with increased doping concentration. Furthermore, the lattice constant increased and then decreased as the applied Se vapor pressure was increased. We suggest that at high Se vapor pressures, the fewer Se vacancies means the formation of Ge substituents is difficult. The conduction type of GaSe doped with 0.5 at % Ge was p-type and the formation of a shallow acceptor level in the bandgap was confirmed for doped GaSe as well as for nominally undoped GaSe. In addition, the carrier concentration at 255 K was reduced to 1/6 of the value of undoped GaSe. The absorption coefficient of GaSe doped with 0.5 at% Ge was lower than that of undoped GaSe below 2.4 THz. This is considered to be due to doped Ge substituents at Se sites forming deep levels, promoting recombination and suppressing free carrier absorption in the low THz frequency range.

Acknowledgement

This work was supported by JSPS Grant-in-Aid for JSPS Research FellowGrant Number JP18J11396.

References

1. Tanabe T, Zhao S, Sato Y and Oyama Y (2017) Effect of adding Te to layered GaSe crystals to increase the van der Waals bonding force. Appl Phys 122: 165105.
2. Hasegawa R, KimuraT, Tanabe T, Nishihara K, Taniyama A, et al. (2018) Analysis of the specific vibration modes of goethite (α-FeOOH) by terahertz spectroscopy and calculations of the vibration frequencies of a single molecule using density functional theory. J Biomed Graph Comput 8: 29-34.
3. Takasuna S, Shiogai J, Matsuzaka S, Kohda M, Oyama Y, et al. (2017) Weak antilocalization induced by Rashba spin-orbit interaction in layered III-VI compound semiconductor GaSe thin films. Phys Rev B 96: 161303.
4. Dmitriev VG, Gurzadyan GG, and Nikogosyan DN (1997) Handbook of Nonlinear Optical Crystals. Springer, Berlin. 166-169.
5. Shi W, Ding YJ (2004) A monochromatic and high-power terahertz source tunable in the ranges of 2.7–38.4 and 58.2–3540 μm for variety of potential applications. Appl Phys Lett 84: 1635.
6. Chen CW, Tang TT, Lin SH, Huang JY, Chang CS, et al. (2009) Optical properties and potential applications of ε-GaSe at terahertz frequencies. J Opt Soc Am B 26: A58-A65.
7. Dezaki H, Tanabe T, Haiyan J, and Oyama Y (2012) Wide Frequency Tunable GaSe Terahertz Emitter under Collinear Phase Matching Condition. Key Eng Mater 500: 58.
8. Zavrazhnov A, Naumov A, Sidey V, Pervov VS (2012) Composition control of low-volatile solids through chemical vapor transport reactions. III. The example of gallium monoselenide: Control of the polytypic structure, non-stoichiometry and properties Thermochimica Acta 527: 118- 124.
9. Tanabe T, Suto K, Nishizawa JI, Sasaki T (2004) Characteristics of terahertz-wave generation from GaSe crystals. J Phys D: Appl Phys 37: 155-158.
10. Nishizawa J, Sasaki T, Oyama Y, Tanabe T (2007) Aspects of Point Defects in Coherent Terahertz-Wave Spectroscopy. Physica B 677: 401-402 .
11. Onai T, Nagai Y, Dezaki H, Oyama Y (2013) Liquid Phase Growth of Bulk GaSe Crystal Implemented with the Temperature Difference Method under Controlled Vapor. J Cryst Growth 380: 18-22.
12. Saito K, Nagai Y, Yamamoto K, Maeda K, Tanabe T, et al. (2014) Terahertz Wave Generation via Nonlinear Parametric Process from ε-GaSe Single Crystals Grown by Liquid Phase Solution Method. OPJ 4: 213-218.
13. Lei N, Sato Y, Tanabe T, Maeda K, Oyama Y (2017) Transition metal doping of GaSe implemented with low temperature liquid phase growth. J Cryst Growth 460: 94-97.
14. Nishizawa J, Kobayashi Y, Okuno Y (1980) Blance method for experiments under controlled vapor pressure. Jpn J Appl Phys 19: 345-352.
15. Baker EH (1968) The vapour pressure and resistivity of selenium at high temperatures. J Che Soc A 1089-1092.
16. Gouskov A, Camassel J,Gouskov L (1982) Growth and characterization of III–VI layered crystals like GaSe, GaTe, InSe, GaSe1-xTex and GaxIn1-xSe. Prog Crystal Growth and Cheract 5: 323-413.